Relativistic effective valence shell Hamiltonian method: Excitation and ionization energies of heavy metal atoms

Rajat K. Chaudhuri
Indian Institute of Astrophysics, Bangalore 560034, India

Karl F. Freed
The James Franck Institute and Department of Chemistry, University of Chicago, Chicago, Illinois 60637

(Received 18 February 2005; accepted 21 March 2005; published online 27 May 2005)

The relativistic effective valence shell Hamiltonian H^v method (through second order) is applied to the computation of the low lying excited and ion states of closed shell heavy metal atoms/ions. The resulting excitation and ionization energies are in favorable agreement with experimental data and with other theoretical calculations. The nuclear magnetic hyperfine constants A and lifetimes τ of excited states are evaluated and they are also in accord with experiment. Some of the calculated quantities have not previously been computed. © *2005 American Institute of Physics*.
[DOI: 10.1063/1.1906206]

I. INTRODUCTION

The accurate estimation of transition energies and nuclear magnetic hyperfine constants for singly ionized metal ions, such as Sr^+, Ba^+, Pb^+, etc., is important because these ions can be used in cold traps as possible frequency standards and in probes of physical phenomena that depart from the prediction of the standard model of physics. For instance, an optical frequency standard based on Sr^+ has recently been developed at the National Physical Laboratory.[1,2] In addition, calculations of the hyperfine coupling constant are relevant to studies of parity nonconservation in atoms because the electroweak interaction is also a short range force such as those determining the hyperfine coupling constant. However, the theoretical determination of the hyperfine coupling constant is, probably, one of the most nontrivial problems in atomic physics because an accurate prediction requires precise incorporation of the strongly entangled relativistic and higher order correlation and relaxation effects.

A variety of many-body methods are available for incorporating relativistic and dynamical electron correlation contributions into descriptions of many-electron systems. One such many-body method, the effective valence shell Hamiltonian H^v method,[3] has been demonstrated in extensive nonrelativistic studies to be capable of providing accurate predictions of transition energies and related properties for complex atomic and molecular systems. This paper describes computations for a series of excitation and ionization energies, magnetic hyperfine constants, and other related properties of the Sr, Ba, and Pb atoms using a relativistic extension of the H^v method and a kinetically balanced basis. While the properties of the Sr^+ and Ba^+ ions have been studied using relativistic single reference second-order many-body perturbation theory[4] (SR-MBPT) and coupled cluster methods,[5] only a few relativistic calculations are available for the corresponding neutral states, in part, because of the greater complexity (i.e., increased nondynamical correlation) involved in the calculation of excited states for the neutral systems. Multireference MBPT methods, on the other hand, are cost effective and can yield highly accurate estimates of ground and excited state properties for systems in which nondynamical correlation is important.

Among the various MR-MBPT approaches, the H^v method has emerged as one of the most powerful and effective tools for high precision calculations of the excitation spectrum. Over the years, the H^v method has been applied successfully to a wide variety of problems involving a host of atomic and molecular systems.[6–14] This paper describes the extension of this H^v scheme for the first time to four-component relativistic calculations in order to assess its performance in a situation where both relativistic and electron correlation effects are important. The present work demonstrates that the relativistic H^v method is also capable of producing accurate transition energies and hyperfine splittings for well known challenging systems. The calculations also highlight the significant contributions from electron correlation to ionization and transition energies.

The following section provides a brief description of the extension of the H^v method to treat relativistic systems. Section III provides the results with comparison to experiments and prior calculations. No previous relativistic computations are available for the excitation energies of the Sr atom or for the hyperfine matrix elements of the Pb^+ ion.

II. THEORETICAL BACKGROUND

A. H^v method

As in conventional many-body perturbation theory, the H^v method[3] begins with the decomposition of the exact Hamiltonian H into the zeroth-order Hamiltonian H_0 and the perturbation V,

$$H = H^{(0)} + V, \tag{1}$$

where $H^{(0)}$ is often constructed as a sum of one-electron Fock operators. The full many-electron Hilbert space of dimension N is then partitioned into a reference space $\mathcal{M}_0$

(also called the active or model space) of dimension $M \ll N$, defined by the projector P, and its orthogonal complement $\mathcal{M}_0^{\perp}$ associated with the projector $Q=1-P$. Once the active space $\mathcal{M}_0$ is defined, a wave operator Ω is introduced that satisfies

$$|\Psi_i\rangle = \Omega|\Psi_i^{(0)}\rangle, \quad i=1,\ldots,M, \tag{2}$$

where $|\Psi_i^{(0)}\rangle$ and $|\Psi_i\rangle$ are the *unperturbed* and *the exact* (full configuration interaction) wave functions (in the given basis) for the ith eigenstate of the Hamiltonian, respectively. The wave operator Ω formally represents the mapping of the reference space $\mathcal{M}_0$ onto the target space $\mathcal{M}$ spanned by the M eigenstates $|\Psi_i\rangle$ and has the properties

$$\Omega P = \Omega, \quad P\Omega = P, \quad \Omega^2 = \Omega. \tag{3}$$

With the aid of the wave operator Ω, the Schrödinger equation for the M eigenstates of the Hamiltonian correlating with the M-dimensional reference space $\mathcal{M}_0$ (often called the P space) of M unperturbed states $|\Psi_i^{(0)}\rangle$, i.e.,

$$H|\Psi_i\rangle = E_i|\Psi_i\rangle, \quad i=1,\ldots,M, \tag{4}$$

is transformed into the generalized Bloch equation

$$H\Omega P = \Omega H \Omega P = \Omega P H_{\text{eff}} P. \tag{5}$$

The Hermitianized effective Hamiltonian through second order can be expressed as

$$H_{\text{eff}} = PHP + \tfrac{1}{2}[PVQ(E_P - H_0)^{-1}QVP + \text{h.c.}], \tag{6}$$

where h.c. denotes the Hermitian conjugate of the preceding term, H_{eff} operates only on a complete active space spanned by a set of valence orbitals $\{v\}$ as defined below, and where E_P is the zeroth-order energy for the P space.

In order to compute the diagonal and off-diagonal matrix elements of an operator A between the normalized full space wave functions Ψ_i within H^v theory, an effective operator A^v is defined as

$$A^v = PAP + \tfrac{1}{2}[\ PVQ(E_P - H_0)^{-1}QAP) + \text{h.c.}]. \tag{7}$$

Once A^v is evaluated, it furnishes all diagonal and off-diagonal matrix elements within the P-space states. Many-body theory techniques are applied to express the matrix elements of A^v directly in the valence orbital basis as

$$A^v = A_c^v + \sum_i A_i^v + \frac{1}{2}\sum_{i,j} A_{ij}^v + \cdots, \tag{8}$$

where A_c^v is the constant core contribution and A_i^v (A_{ij}^v) is a one(two)-electron effective operator in the valence orbital basis $\{v\}$.

Apart from the reference (P) space, the only variability in all MR-MBPT methods lies in the choice of orbitals, orbital energies, and the definition of the zeroth-order Hamiltonian H_0 since the perturbation approximation is completely determined by these choices. Generally, the zeroth-order Hamiltonian is prescribed as a sum of one-electron operators,

$$H_0'(i) = \sum_c |\phi_c\rangle\epsilon_c\langle\phi_c| + \sum_v |\phi_v\rangle\epsilon_v\langle\phi_v| + \sum_e |\phi_e\rangle\epsilon_e\langle\phi_e|, \tag{9}$$

in terms of the core c, valence v, and excited e orbitals and their corresponding orbital energies ϵ_c, ϵ_v, and ϵ_e, respectively. At this point, we emphasize that unlike traditional MR-MBPT treatments, the H^v method and its first-order approximation based on retention of only the PHP term, called the "improved virtual orbital complete active space configuration interaction" (IVO-CASCI) method, use *multiple* Fock operators to define the valence orbitals.[10,15,16] In this scheme, all the valence orbitals and orbital energies are obtained from $V^{(N-1)}$ potentials and, therefore, are on an equal footing energetically, as opposed to the unbalanced use of a mixture of Hartree–Fock or Dirac–Fock (DF) occupied and virtual orbitals to construct the valence space in many multireference methods. The H^v method defines the zeroth-order Hamiltonian H_0 in terms of the one-electron operator,

$$H_0(i) = \sum_c |\phi_c\rangle\epsilon_c\langle\phi_c| + \sum_v |\phi_v\rangle\overline{\epsilon_v}\langle\phi_v| + \sum_e |\phi_e\rangle\epsilon_e\langle\phi_e|, \tag{10}$$

where in order to improve the perturbative convergence,[17–19] the average valence orbital energy $\overline{\epsilon_v}$ in Eq. (10) is obtained from the original set of valence orbital energies by the democratic averaging,

$$\overline{\epsilon_v} = \frac{\sum_i^{N_v} \epsilon_i}{N_v}, \tag{11}$$

with N_v being the number of valence orbitals spanning the complete active P space. Prior applications of the IVO-CASCI method demonstrate that it produces comparable accuracy to complete active space self-contained field (CASSCF) treatments with the same choice of valence space (of course, using different valence orbitals) but with considerably reduced computer time since no iterations are necessary beyond an initial ordinary self-consistent field calculation.[20,21]

Because the IVOs play a central role in this perturbative scheme, we briefly outline their generation. More detailed discussion is presented elsewhere.[20,21] The IVO-CASCI procedure first determines the occupied and unoccupied DF molecular orbitals (MOs) by diagonalizing the four-component DF matrix ${}^1F_{lm}$ for the reference state,

$${}^1F_{lm} = \langle\phi_l|h + \sum_{k=1}^{\text{occ}} (2J_k - K_k)|\phi_m\rangle = \delta_{lm}\epsilon_l, \tag{12}$$

where l and m designate any (occupied or unoccupied) DF MO and ϵ_l is the corresponding DF orbital energy. The IVOs are determined variationally by minimizing the energies of the low lying singly excited states $\Psi_{\alpha\to\mu}$ with respect to a new set of MOs $\{\chi\}$ (where α is usually taken as the highest occupied MO). However, to ensure orbital orthogonality and applicability of Brillouin's theorem, $\{\chi\}$ are expressed in terms of the DF orbitals $\{\phi\}$ as

$$\chi_\alpha = \sum_{i=1}^{\text{occ}} a_{\alpha i}\phi_i, \quad \chi_\mu = \sum_{u=1}^{\text{unocc}} c_{\mu u}\phi_u, \tag{13}$$

involving separate sums over occupied and unoccupied orbitals in the DF approximation for the reference state. The problem is further simplified by setting $\{\chi_\alpha\}$ to be occupied orbitals of the reference DF configuration. With this choice, the coefficients $c_{\mu u}$ in Eq. (13) can be determined directly from the matrix eigenvalue equation $F'C=C\Gamma$, where

$$F'_{vw} = {}^1F_{vw} - \delta F^{\alpha}_{vw}, \tag{14}$$

$$\delta F^{\alpha}_{vw} = \langle \chi_v | J_\alpha | \chi_w \rangle. \tag{15}$$

Second-order H^v calculations are very rapidly implemented. The most time consuming step generally involves the computation of the effective three-body interactions, symmetry inequivalent six-index quantities whose number scales as the product of the sixth power of the number (N_v) of valence orbitals and the sum of the number of core and excited orbitals (of course, not including the frozen "positron" core orbitals). The maximum size of the reference space used here $(N_v=6)$ and the high atomic symmetry helps keep even this step very rapid with large basis sets. Moreover, because of the Fock space formulation, once H^v has been evaluated, energies are readily computed for both the neutral and positive ion valence states.

B. Relativistic theory

The relativistic effective valence shell Hamiltonian H^v method is applied to compute excitation energies for the Sr and Ba atoms and ionization energies for the Sr, Ba, and Pb atoms. The Jucys–Levinson–Vanagas theorem[22] is employed to decompose each Goldstone diagram contributing to Eq. (9) into the product of an angular momentum diagram and a reduced matrix element. This procedure simplifies the computational complexity of the DF and relativistic H^v equations. In the calculations, the problem of "continuum dissolution" is formally avoided by introducing projection operators to select the positive energy states or, in other words, by excluding all summations over negative energy states.[23]

The Dirac–Coulomb Hamiltonian for the many-electron system is written as

$$H = \sum_{i=1}^{N} [c\vec{\alpha}_i \cdot \vec{p}_i + (\beta_i - 1)mc^2 + V_{\text{nuc}}(r_i)] + \frac{1}{2}\sum_{i\neq j} \frac{e^2}{|\vec{r}_i - \vec{r}_j|} \tag{16}$$

in terms of the customary Dirac operators $\vec{\alpha}$ and β that are represented by the matrices

$$\vec{\alpha} = \begin{pmatrix} 0 & \vec{\sigma} \\ \vec{\sigma} & 0 \end{pmatrix}, \quad \beta = \begin{pmatrix} I & 0 \\ 0 & -I \end{pmatrix}, \tag{17}$$

where $\vec{\sigma}$ denotes the Pauli matrices and I is the 2×2 unit matrix. The simplest choice for $V_{\text{nuc}}(r)$ is a point source of electric field with a Coulomb potential of the form,

$$V_{\text{nuc}}(r) = -\frac{Z}{r}, \tag{18}$$

where Z is the atomic number. However, this nuclear model introduces a nonphysical singularity which is known to influence the convergence properties of the finite basis set expansion, particularly if a Gaussian-type basis set is employed.[24] Further, the nuclear volume isotope shift, observed in heavy atoms, reflects the finite size of the nucleus with the nuclear charge distribution depending upon the atomic number A. Among the various nuclear models, the "Fermi nucleus" is a popular choice of nuclear model without a sharp cutoff. Experimental studies suggest that the nuclear charge distribution posses a "skin" of finite thickness across which the nuclear charge density falls to zero as in the Fermi nucleus model. The present work uses the Fermi nucleus model in which the charge density inside the nucleus varies as

$$\rho(r) = \rho_0\{1 + \exp[(r-b)/a]\}^{-1}, \tag{19}$$

where ρ_0 is a constant (depending on Z) (Ref. 25) and b is the cutoff radius (also called "half-density radius") at which $\rho(b)=\rho_0/2$. The parameter a is related to the nuclear skin thickness t by

$$a = t/(4\ln 3), \tag{20}$$

where $t=2.30$ fm for the Fermi nucleus model.[26]

The relativistic orbitals are expressed in the form

$$\begin{pmatrix} r^{-1}P_{n\kappa}(r)\chi_{\kappa m}(\theta,\phi) \\ ir^{-1}Q_{n\kappa}(r)\chi_{-\kappa m}(\theta,\phi) \end{pmatrix}, \tag{21}$$

where $r^{-1}P_{n\kappa}(r)$ and $r^{-1}Q_{n\kappa}(r)$ are the large and small components of the radial wave functions, respectively, that satisfy the orthogonality condition

$$\int_0^\infty dr[P_{n\kappa}(r)^* P_{m\kappa}(r) + Q_{n\kappa}(r)^* Q_{m\kappa}(r)] = \delta_{mn}. \tag{22}$$

The quantum number κ classifies the orbital according to symmetry and is given by

$$\kappa = \mp\left(j \pm \tfrac{1}{2}\right), \tag{23}$$

where l is the orbital quantum number and $j=l\pm\frac{1}{2}$ is the total angular quantum number. The spinors $\chi_{\kappa m}(\theta,\phi)$ are written as

$$\chi_{\kappa m}(\theta,\phi) = \Sigma_{\sigma=\pm 1/2} C\left(l\tfrac{1}{2}, m-\sigma, \sigma\right) Y_{l,m-\sigma}(\theta,\phi)\,\eta_\sigma, \tag{24}$$

where $C(l\frac{1}{2}, m-\sigma, \sigma)$ and $Y_{l,m-\sigma}(\theta,\phi)$ represent the Clebsch–Gordon coefficients and the normalized spherical harmonics, respectively, and η_σ is a two-component spinor.

The large and small component radial wave functions are expressed as linear combinations of basis functions

$$P_{n\kappa}(r) = \sum_{p=1}^{N} C^L_{\kappa p} g^L_{\kappa p}(r), \quad Q_{n\kappa}(r) = \sum_{p=1}^{N} C^S_{\kappa p} g^S_{\kappa p}(r), \tag{25}$$

where the summation index p runs over the number of basis functions N and $g^L_{\kappa p}$ $(g^S_{\kappa p})$ and $C^L_{\kappa p}$ $(C^S_{\kappa p})$ are the basis functions and expansion coefficients for the large (small) compo-

nents, respectively. The basis functions employed in these calculations are Gaussian-type orbitals (GTOs) of the form

$$g^L_{\kappa p}(r) = N^L_p r^{n_\kappa} e^{-\alpha_p r^2} \tag{26}$$

with

$$\alpha_p = \alpha_0 \beta^{p-1}, \tag{27}$$

where α_0 and β are user defined constants, n_κ specifies the orbital symmetries (1 for s, 2 for p, etc.), and N^L_p is the normalization factor for the large component. The small component normalization factor is obtained by imposing the *kinetic balance* condition

$$g^S_{\kappa p}(r) = N^S_p \left(\frac{d}{dr} + \frac{\kappa}{r} \right) g^L_{\kappa p}(r), \tag{28}$$

where

$$N^S_p = \sqrt{\frac{\alpha_p}{2n_\kappa - 1}[4(\kappa^2 + \kappa - n_\kappa) - 1]}. \tag{29}$$

The ground and excited state properties of Sr, Ba, and their positive ions are computed using $37s33p28d12f5g$ GTOs with $\alpha_0 = 0.005\,25$ and $\beta = 2.25$. For the Pb^+ ion, we employ $38s35p30d25f20g$ GTOs with $\alpha_0 = 0.008\,25$ and $\beta = 2.73$.[27]

III. RESULTS AND DISCUSSION

The choice of reference space plays a central role in all multireference perturbative methods. This choice is also the most difficult portion of all MR-MBPT calculations as it can affect the accuracy of the computed spectroscopic constants and state energies. However, the choice of reference space is fairly straightforward for Sr, Ba, and Pb. The ground states of the Sr and Ba neutral atoms contain only two electrons in the outermost occupied ns orbital ($n=5$ for Sr and $n=6$ for Ba) whose orbital energy is well separated from the remaining occupied orbital energies. Since the improved virtual orbitals $6s(\epsilon_{6s} = -0.1219$ a.u.), $5p_{1/2}(\epsilon_{5p_{1/2}} = -0.1439$ a.u.), $5p_{3/2}(\epsilon_{5p_{3/2}} = -0.1414$ a.u.), $4d_{3/2}(\epsilon_{4d_{3/2}} = -0.1107$ a.u.), and $4d_{5/2}(\epsilon_{4d_{3/2}} = -0.1104$ a.u.) of Sr are quasidegenerate, these orbitals are also included in reference space. Using similar arguments, the $7s$, $6p_{1/2}$, $6p_{3/2}$, $5d_{3/2}$, and $5d_{5/2}$ orbitals of Ba are included in the H^v reference space for Ba. Finally, the H^v reference space for Pb is constructed by allocating two electrons to the $6p_{1/2}$ and $6p_{3/2}$ orbitals in all possible ways because of the larger s-p energetic separation in this heavier atom. Calculations for Pb are limited to the positive ion because the treatment of the neutral atom would require a larger reference space ($N_v = 10$ or 12) that is no longer quasidegenerate and that therefore should be studied using third order H^v relativistic calculations, which are not yet possible.

A. Excitation energies

Table I compares experimental[28–31] and calculated low lying excitation energies of Sr and Ba. Included also are coupled cluster (CC) calculations for Ba. The H^v transition energies for the Sr and Ba atoms are in excellent agreement with experiment. The maximum error in the estimated excitation energy for Sr is only 159 cm^{-1} (or 0.7%) for the $^1P_1$ state. The H^v method also provides a fairly accurate estimate of the $^3P_0 \rightarrow {}^3P_1$ and $^3P_1 \rightarrow {}^3P_2$ transition energies, which deviate by only 37 cm^{-1} and 14 cm^{-1}, respectively, from experiment. The Ba transition energies from the H^v calculations are also quite accurate, except for the $^3P_0 \rightarrow {}^3P_1$ and $^3P_1 \rightarrow {}^3P_2$ transitions, which are off by $\sim$100 cm^{-1}.

TABLE I. Low lying transition energies (in cm^{-1}) for the Sr and Ba atoms.

Atom	State	Dominant configuration(s)	H^v	CC[a]	Experiment[b]
Sr					
	$^3P_0$	$5s5p$	14 428		14 327
	$^3P_1$	$5s5p$	14 582		14 514
	$^3P_2$	$5s5p$	14 980		14 898
	$^1P_1$	$5s5p$	21 539		21 698
Ba					
	$^3P_0$	$6s6p$	12 235	12 503	12 266
	$^3P_1$	$6s6p$	12 523	12 882	12 637
	$^3P_2$	$6s6p$	12 289	13 792	13 514
	$^1P_1$	$6s6p$	18 014	18 455	18 060

[a]Reference 5.
[b]References 26–30.

Table I indicates, on the other hand, that the error in the estimated CC (H^v) energies for the Ba atom $^3P_0$, $^2P_1$, and $^3P_2$ states are 237(31) cm^{-1}, 245(114) cm^{-1}, and 278(225) cm^{-1}, respectively. Since the difference between the maximum deviation and the minimum deviation from experiment for the CC calculations of the ^3P state energies is less (41 cm^{-1}) than that for the H^v treatment (194 cm^{-1}), the CC offers a more accurate description of the fine structure splittings for the ^3P states of Ba, even though the CC transition energies for these states are less accurate than the corresponding H^v estimates. [The average error in the CC excitation energies for the Ba atom is 2.0%, while that for the H^v case is only 0.7%.] However, it should be emphasized that the CC calculations include contributions from the Breit interactions that are omitted in our calculations. Moreover, both computations (CC and H^v) employ different basis sets. We believe that the inaccuracy in our computed fine structure splittings for the ^3P states of Ba mainly arises due to the absence of higher order correlation contributions and the Breit interaction in our calculations, and efforts are underway to enable including these effects.

B. Valence electron ionization energies

Table II compares the H^v calculations for low lying valence electron ionization energies of Sr^+, Ba^+, and Pb^+ with those computed using single reference MBPT and CC methods and with experiments.[28] The H^v method estimates the $^2P_{1/2} \rightarrow {}^2P_{3/2}$ energy gap (the fine structure splitting which is labeled as FS in Table II) of Sr more accurately than the SR-MBPT. Table II further shows that the average error in the computed H^v energies (0.13%) is less than those from the SR-MBPT (0.48%) and comparable to CC (0.12%) treatments. A careful analysis indicates that only the [Kr]$5s$ H^v

TABLE II. Theoretical and experimental valence electron ionization energies (in cm^{-1}) and fine structure splittings (FS) of Sr^+, Ba^+, and Pb^+ ions.

Ion	State	H^v	MBPT[4]	CC	Experiment[a]
Sr^+	$^2S_{1/2}$ $(5s)$	89 248	89 631	89 126[b]	88 964
	$^2P_{1/2}$ $(5p_{1/2})$	65 219	65 487	65 309[b]	65 249
	$^2P_{3/2}$ $(5p_{3/2})$	64 403	64 663	64 499[b]	64 448
	FS	816	824	810	801
	Average error	0.13%	0.48%	0.12%	
Ba^+	$^2S_{1/2}$ $(6s)$	81 734	81 882	80 871[c]	80 687
	$^2P_{1/2}$ $(6p_{1/2})$	60 481	60 887	60 475[c]	60 425
	$^2P_{3/2}$ $(6p_{3/2})$	58 759	59 139	58 768[c]	58 735
	FS	1 722	1 748	1 707	1 690
	Average error	0.48%	0.98%	0.12%	
Pb^+	$^2P_{1/2}$ $(6p_{1/2})$	122 382	121 898	120077[d]	121 208
	$^2P_{3/2}$ $(6p_{3/2})$	108 353	108 041	106377[d]	107 123
	FS	14 029	13 857	13700	14 085
	Average error	1.06%	0.71%	0.82%	

[a]Reference 28.
[b]Referene 34.
[c]Reference 5.
[d]Reference 27.

valence electron removal energy is slightly poorer (off by 284 cm^{-1}) compared to the CC estimate (off by 162 cm^{-1}). This error also affects the H^v calculation of the fine structure splitting.

The H^v valence electron ionization energies of Ba^+ are reasonably close to experiment, except for the $^2S_{1/2}$ state which is dominated by the [Xe]6*s* configuration state function. On the other hand, the Ba^+ fine structure splitting for the $^2P_{1/2}\rightarrow{}^2P_{3/2}$ states is quite close to experiment (off by only 32 cm^{-1}) and to the CC estimate. The overall error in the computed H^v energies for Ba^+ is 0.48% which is better than the SR-MBPT (0.98%) but not as good as the CC (0.12%) computations. However, the very inexpensive nature (roughly an order of magnitude faster) of second-order H^v calculations compared to the computational cost involved in the CC calculations renders this minuscule error quite acceptable.

For the Pb^+ ion, the computed CC and SR-MBPT valence electron ionization energies are more accurate than the corresponding H^v values. On the other hand, the H^v fine structure splitting for the $^2P_{1/2}(6p_{1/2})\rightarrow{}^2P_{3/2}(6p_{3/2})$ states of Pb^+ is more accurate than the CC and SR-MBPT treatments. At this juncture, we note that a precise determination of the $^2P_{1/2}\rightarrow{}^2P_{3/2}$ transition energy is necessary for an accurate prediction of the lifetime of the $^2P_{3/2}$ state because the $E_{6p1/2}-E_{6p3/2}$ energy difference appears raised to the third (fifth) power for the $M1(E2)$ allowed $6p_{1/2}\rightarrow 6p_{3/2}$ transition in Pb^+.

C. Nuclear magnetic hyperfine constant *A* and lifetime τ

The nuclear magnetic hyperfine constant and transition dipole/quadrupole matrix elements are computed using the second-order (in the Coulomb perturbation) H^v wave functions and thus contain contributions such as those depicted in Fig. 1. Tables III–VI present the theoretically determined nuclear magnetic hyperfine constants and life times for the excited states of Sr^+, Ba^+, and Pb^+. Also included are other computations and experimental data for comparison. The reduced matrix elements for the magnetic hyperfine *A*, electric dipole *E*1, electric quadrupole *E*2, and magnetic dipole *M*1 matrix elements are presented in Appendixes A and B.

Table III indicates that our predicted nuclear magnetic hyperfine constants are in general agreement with experiments, except for the 6*s* ($^2S_{1/2}$) and 6*p* ($^2P_{3/2}$) states of Ba^+ and Pb^+, for which the CC treatments are also not very ac-

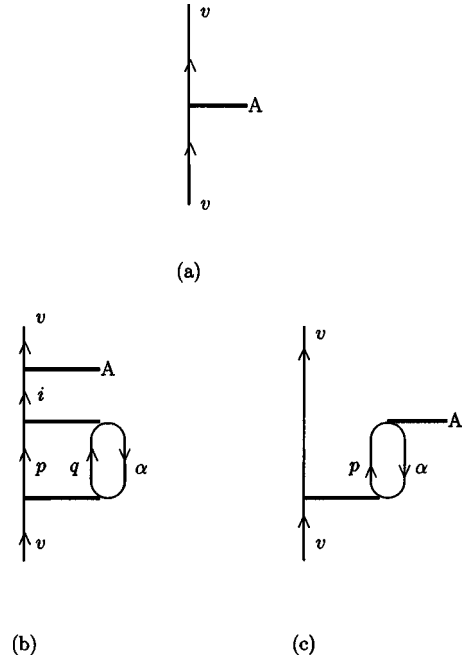

FIG. 1. Some representative Goldstone diagrams that contribute to the nuclear magnetic hyperfine coupling constant *A*. The particle orbitals are labeled by $p,q,\ldots$, etc. Occupied orbitals are represented by $\alpha,\beta,\ldots$, etc. The active (valence) and inactive orbitals are denoted by v and i, respectively.

TABLE III. Nuclear magnetic hyperfine constant (in megahertz) of the ground and low lying excited states Sr^+, Ba^+, and Pb^+.

Ion	State	Present work	CC	Experiment
Sr^+				
	$^2S_{1/2}$ $(5s)$	1 005.74	1 000[a]	1 000.47[b]
	$^2P_{1/2}$ $(5p_{1/2}s)$	167.96	177[a]	
	$^2P_{3/2}$ $(5p_{3/2})$	34.82	35.3[a]	36.8[c]
Ba^+				
	$^2S_{1/2}$ $(6s)$	4 165.20	4 072.83[d]	4 018[e]
	$^2P_{1/2}$ $(6p_{1/2})$	736.28	736.98[d]	742.04[e]
$^2P_{3/2}$ $(6p_{3/2})$		131.18	130.94[d]	126.9[e]
Pb^+	$^2P_{1/2}$ $(6p_{1/2})$	12 972.42	12 903.7[f]	13 000[g]
	$^2P_{3/2}$ $(6p_{3/2})$	512.52	623.2[f]	583[g]

[a]Reference 34.
[b]Reference 35.
[c]Reference 36.
[d]Reference 37.
[e]Reference 38.
[f]Reference 39.
[g]Reference 40.

curate. It is evident from Tables III and IV that the overall correlation contribution to magnetic hyperfine matrix elements for the $6p$ $(^2P_{3/2})$ state of Pb^+ should be negative as the zeroth-order DF approximation overestimates the magnetic hyperfine A value. Thus, the overall correlation contribution to the magnetic hyperfine coupling constant for the $^2P_{3/2}$ states of Sr^+ and Ba^+ must be positive. The present calculations clearly exhibit this anticipated trend. The large negative contribution from core polarization [Fig. 1(c)] may appear to be quite unusual, but this same trend is found for the $6p_{3/2}$ $(^2P_{3/2})$ state of Tl (Ref. 32) and the $3d_{5/2}$ $(^2D_{5/2})$ state of Ca^+.[33] The CC calculation[33] shows that higher order contributions are necessary for accurately describing the magnetic hyperfine matrix elements for the $3d_{5/2}$ $(^2D_{5/2})$ state of Ca^+.[33] The accuracy of the $6p_{3/2}$ $(^2P_{3/2})$ state A value for Pb^+ strongly suggests that the inclusion of higher order correlation corrections is likewise necessary for an accurate determination of A when the core-polarization contribution is large and negative with respect to the DF value.

The lifetime for the excited states of Sr^+ and Ba^+ are computed from the $E1$ transition probabilities, while the lifetime of the $6p$ $(^2P_{3/2})$ state of Pb^+ is estimated from the $M1$ and $E2$ transition probabilities. The MBPT lifetimes for the excited states of Sr^+ and Ba^+ reported by Guet *et al.* are quite accurate but are determined using experimental transition energies (λ) and semiempirically adjusted electric dipole transition matrix elements (D). On the other hand, the accuracy

TABLE IV. Contributions of relatively large matrix elements (in megahertz) to the total magnetic hyperfine constant for $^2P_{3/2}$ $(np_{3/2})$ states of Sr^+, Ba^+, and Pb^+ (n=5 for Sr and 6 for Ba and Pb).

Terms	Sr^+	Ba^+	Pb^+
Dirac–Fock [Fig. 1(a)]	21.33	71.88	918.37
Pair correlation [Fig. 1(b)]	4.80	22.12	91.72
Core polarization [Fig. 1(c)]	8.02	30.32	−787.19

TABLE V. Lifetimes τ (in nanoseconds) of low lying excited states of Sr^+ and Ba^+ ($E1$). Entries in parentheses are calculated from experimental transition energies and semiempirically adjusted transition dipole ($E1$) matrix elements.

Ion	State	H^v	Other calculation	Experiment
Sr^+				
	$5p_{1/2}$	7.47	7.08(7.48)[a]	7.47±0.07[b]
	$5p_{3/2}$	6.888	6.39(6.74)[a]	6.69±0.07[c]
Ba^+				
	$6p_{1/2}$	7.89	7.25(7.99)[a]	7.92±0.08[b]
	$5p_{3/2}$	5.98	5.84(6.39)[a]	6.31±0.02[b]

[a]Reference 4.
[b]Reference 41.
[c]Reference 42.

of the computed lifetimes degrade when their theoretical transition energies and dipole matrix are used.

The H^v lifetimes for the excited states of Sr^+ and Ba^+ in Table V are evaluated from the H^v transition energies and dipole matrix elements. The $5p$ $(^2P_{1/2})$ state lifetime of Sr^+ is well reproduced by the H^v method. The accuracy of our computed lifetime for the $5p$ $(^2P_{3/2})$ state of Sr^+ is not as good as that for the $5p$ $(^2P_{1/2})$ state mainly due to the errors in the $5p_{3/2}\rightarrow 4d_{3/2}$ and $5p_{3/2}\rightarrow 4d_{5/2}$ computed transition energies and the corresponding dipole matrix elements. The $6p$ $(^2P_{3/2})$ state lifetime of Pb^+ is computed using the H^v transition energy and transition matrix elements ($M1$ and $E2$) and is quite accurate compared to the CC value[27] (see Table VI). Since the H^v energy for the $6p_{1/2}\rightarrow 6p_{3/2}$ transition is also quite accurate, we believe that both $M1$ and $E2$ transition matrix elements are likewise very accurate.

IV. CONCLUDING REMARKS

The relativistic effective valence shell Hamiltonian H^v method is described and applied in second order to the low lying states of the Sr and Ba atoms and to the positive ions of Sr, Ba, and Pb. Highly satisfactory results are obtained for the transition energies, valence electron ionization potentials, magnetic hyperfine constant, and the lifetime of low lying excited states of the Sr^+, Ba^+, and Pb^+ ions. To our knowledge, no prior theoretical data are available for the transition energies of Sr and the magnetic hyperfine constant of Pb^+. The accuracy achieved with the computationally inexpensive second-order H^v scheme is comparable (even better in some cases) to the much more computer intensive CC scheme. Note, however, that it remains to be determined whether the inclusion of Breit interaction in our calculations improves accuracy of these computed quantities, especially for Pb. Work in this direction is in progress.

TABLE VI. Lifetime τ (in seconds) of $6p_{3/2}$ $(^2P_{3/2})$ excited state of Pb^+.

Ion	State	H^v	CCSD[a]	Expt.[b]
Pb^+				
	$6p_{3/2}$	0.0409	0.0440	0.0412±0.0007

[a]Reference 27.
[b]Reference 31.

APPENDIX A: NUCLEAR MAGNETIC HYPERFINE MATRIX ELEMENTS

The relativistic nuclear hyperfine interaction is given by[43]

$$H_{\mathrm{hfs}} = \sum_k M^{(k)} \cdot T^{(k)}, \tag{A1}$$

where $M^{(k)}$ and $T^{(k)}$ are spherical tensor operators of rank k, representing the nuclear and electronic parts, respectively, of the interaction. In first-order perturbation theory, the hyperfine energies $W(J)$ of the fine structure states $|JM_J\rangle$ are the expectation values of H_{nfs},

$$W(J) = \langle IJFM_F|\sum_k M^{(k)} \cdot T^{(k)}|IJFM_F\rangle = \sum_k (-1)^{I+J+F}\begin{pmatrix} I & J & F \\ J & I & K \end{pmatrix}\langle I||M^{(k)}||I\rangle\ \langle J||T^{(k)}||J\rangle. \tag{A2}$$

For the magnetic dipole case $k=1$, the nuclear dipole moment μ_I (in units of the nuclear magnetron μ_N) is defined as

$$\mu_I\mu_N = \langle II||M_0^{(1)}||II\rangle = \begin{pmatrix} I & 1 & I \\ -I & 0 & I \end{pmatrix}\langle I||M^{(1)}||I\rangle, \tag{A3}$$

while the operator $T_q^{(1)}$ is given by[44]

$$T_q^{(1)} = \sum t_q^{(1)} = \sum_j -ie(8\pi/3)^{1/2} r_j^{-3}\alpha_j Y_{1q}^{(0)}(\hat{r}_j), \tag{A4}$$

in which α is the Dirac matrix and Y_{kq}^{λ} represents a spherical harmonic. Defining the magnetic dipole hyperfine constant A by

$$A = \mu_N(\mu_I/I)\frac{\langle J||T^{(1)}||J\rangle}{\sqrt{J(J+1)(2J+1)}}, \tag{A5}$$

the magnetic dipole hyperfine energy W is then obtained as

$$W = A\langle IJ\rangle. \tag{A6}$$

The single-particle reduced matrix element of the electronic part is given by

$$\langle\kappa||t_q^{(1)}||\kappa'\rangle = -\langle\kappa||C_q^{(1)}||\kappa'\rangle(\kappa+\kappa') \times\int dr\frac{[P_\kappa(r)Q_{\kappa'}(r) + Q_\kappa(r)P_{\kappa'}(r)]}{r^2}, \tag{A7}$$

where

$$\langle\kappa||C_q^{(k)}||\kappa'\rangle = (-1)^{j+1/2}\begin{pmatrix} j & k & j' \\ 1/2 & 0 & -1/2 \end{pmatrix} \times\sqrt{(2j+1)(2j'+1)}\,\pi(l,k,l') \tag{A8}$$

and

$$\pi(i,j,k) = \begin{cases} 1 & \text{if } i+j+k = \text{even} \\ 0 & \text{otherwise.} \end{cases} \tag{A9}$$

APPENDIX B: ELECTRIC DIPOLE (*E*1), QUADRUPOLE (*E*2), AND MAGNETIC DIPOLE (*M*1) ALLOWED TRANSITION PROBABILITIES

The transition probabilities $A_{f\leftarrow i}$ for the electric dipole $E1$, electric quadrupole $E2$, and magnetic dipole $M1$ allowed transitions (in s^{-1}) are given by[45]

$$A_{f\leftarrow i}^{E1} = \frac{2.0261\times10^{18}}{g_k\lambda^3}S_{f\leftarrow i}^{E1}, \tag{B1}$$

$$A_{f\leftarrow i}^{E2} = \frac{1.1199\times10^{18}}{g_k\lambda^5}S_{f\leftarrow i}^{E2}, \tag{B2}$$

$$A_{f\leftarrow i}^{M1} = \frac{2.6973\times10^{13}}{g_i\lambda^3}S_{f\leftarrow i}^{M1}, \tag{B3}$$

respectively. Here, λ is the transition energy in angstroms and $g_k \equiv (2J+1)$ is degeneracy of the upper level. The quantities $S_{f\leftarrow i}^{E1}$, $S_{f\leftarrow i}^{E2}$, and $S_{f\leftarrow i}^{M1}$ are the $E1$, $E2$, and $M1$ line strengths (in atomic units), respectively. The line strengths $S_{f\leftarrow i}^{(EL/M1)}$ are defined by

$$S_{f\leftarrow i}^{EL/M1} = D_{if}^{EL/M1}\times D_{fi}^{EL/M1}, \tag{B4}$$

where the electric dipole (and quadrupole) D_{fi}^{EL} and magnetic dipole matrix elements D_{fi}^{M1} are given by

$$D_{fi}^{EL} = C^L(f,i)\int dr[P_f(r)P_i(r) + Q_f(r)Q_i(r)]r^L + O(\alpha^2) \tag{B5}$$

and

$$D_{fi}^{M1} = C^{M1}(f,i)\frac{(\kappa_f+\kappa_i)}{\alpha}\int dr[P_f(r)Q_i(r) + Q_f(r)P_i(r)]r + O(\alpha^2), \tag{B6}$$

with

$$C^L(f,i) = (-1)^{j_f+1/2}\begin{pmatrix} j_f & L & j_i \\ 1/2 & 0 & -1/2 \end{pmatrix}\sqrt{(2j_f+1)(2j_i+1)} \tag{B7}$$

and

$$C^{M1}(f,i) = (-1)^{j_f+1/2}\begin{pmatrix} j_f & 1 & j_i \\ 1/2 & 0 & -1/2 \end{pmatrix}\sqrt{(2j_f+1)(2j_i+1)}. \tag{B8}$$

Here, j, κ, and α are the total angular momentum, relativistic angular momentum $[\kappa = \pm(j+1/2)]$, and fine structure constant, respectively.

Once the transition probability is known, the lifetime can be evaluated through the relation

$$\tau = \frac{1}{A}. \tag{B9}$$

[1] M. G. Boshier, G. P. Barwood, G. Huang, and H. A. Klein, Appl. Phys. B: Lasers Opt. **71**, 51 (2000).
[2] G. Barwood, K. Gao, P. Gill *et al.* IEEE Trans. Instrum. Meas. **50**, 543 (2001).
[3] K. F. Freed, *Lecture Notes in Chemistry* (Springer, Berlin, 1989), Vol. 52, p. 1, and references therein.

[4]C. Guet and W. R. Johnson, Phys. Rev. A **44**, 1531 (1991).
[5]E. Eliav and U. Kaldor, Phys. Rev. A **53**, 3050 (1996).
[6]K. F. Freed, in *Lecture Notes in Chemistry*, edited by U. Kaldor (Springer, Berlin, 1989), Vol. 52, p. 1.
[7]R. L. Graham and K. F. Freed, J. Chem. Phys. **96**, 1304 (1992).
[8]C. M. Martin and K. F. Freed, J. Chem. Phys. **100**, 7454 (1994).
[9]J. E. Stevens, K. F. Freed, F. Arendt, and R. L. Graham, J. Chem. Phys. **101**, 4832 (1994).
[10]J. P. Finley and K. F. Freed, J. Chem. Phys. **102**, 1306 (1995).
[11]J. E. Stevens, R. K. Chaudhuri, and K. F. Freed, J. Chem. Phys. **105**, 8754 (1996).
[12]R. K. Chaudhuri and K. F. Freed, J. Chem. Phys. **119**, 5995 (2003).
[13]R. K. Chaudhuri and K. F. Freed, J. Chem. Phys. (in press).
[14]R. K. Chaudhuri, Int. J. Mol. Sci. **4**, 586 (2003).
[15]X.-C. Wang and K. F. Freed, J. Chem. Phys. **86**, 2899 (1987).
[16]R. L. Graham and K. F. Freed, J. Chem. Phys. **96**, 1304 (1992).
[17]R. K. Chaudhuri, J. P. Finley, and K. F. Freed, J. Chem. Phys. **106**, 4067 (1997).
[18]J. P. Finley, R. K. Chaudhuri, and K. F. Freed, J. Chem. Phys. **103**, 4990 (1995).
[19]J. P. Finley, R. K. Chaudhuri, and K. F. Freed, Phys. Rev. A **54**, 343 (1996).
[20]D. M. Potts, C. M. Taylor, R. K. Chaudhuri, and K. F. Freed, J. Chem. Phys. **114**, 2592 (2001).
[21]R. K. Chaudhuri, K. F. Freed, S. A. Abrash, and D. M. Potts, J. Mol. Struct.: THEOCHEM **547**, 83 (2001).
[22]A. P. Jucys (Yutsis), I. B. Levinson, and V. V. Vanagas, Mathematical Apparatus of the Theory Angular Momentum (Israel Program for Scientific Translation, Jerusalem), 1962.
[23]J. Sucher, Int. J. Quantum Chem. **24**, 3 (1984).
[24]J. D. Morgan, in *New Methods in Quantum Theory*, NATO ASI Series, Vol. 3 edited by C. A. Tsipis, V. S. Popov, D. R. Herschback, and J. S. Avery (Kluwer, Dordrecht), Vol. 3, p. 311.
[25]K. G. Dyall and K. Faegri, Chem. Phys. Lett. **201**, 27 (1993).
[26]F. A. Parpia, J. Phys. B **31**, 1409 (1998).
[27]B. K. Sahoo, S. Majumder, R. K. Chaudhuri, B. P. Das, and D. Mukherjee, J. Phys. B **37**, 3409 (2004).
[28]C. E. Moore, *Atomic Energy Levels*, Natl. Bur. Stand. Ref. Data Ser., Natl. Bur. Stand. (U.S.) Circ. No. 35 (U.S. GPO, Washington, D.C., 1971), Vol. 1.
[29]G. Ferrari, P. Cancio, R. Drullinger, G. Giusfredi, M. Prevedelli, C. Toninelli, and G. M. Tino, Phys. Rev. Lett. **91**, 243002 (2003).
[30]S. G. Schmelling and G. O. Brink, Phys. Rev. A **12**, 2498 (1975); H. P. Palenius, Phys. Lett. **56A**, 451 (1976); J. R. Rubbmark, S. A. Borgstrom, and K. Bockasten, J. Phys. B **10**, 1803 (1977).
[31]A. Roth, C. H. Gerz, D. Wilsodorf, and G. Werth, Z. Phys. D: At., Mol. Clusters **11**, 283 (1989).
[32]R. K. Chaudhuri (unpublished).
[33]B. K. Sahoo, R. K. Chaudhuri, B. P. Das, S. Majumder, H. Merlitz, U. Sinha Mahapatra, and D. Mukherjee, J. Phys. B **36**, 1899 (2003).
[34]A. Mårtensson-Pendrill, J. Phys. B **35**, 917 (2002).
[35]G. P. Barwood, K. Gao, P. Gill, G. Huang, and H. A. Klein, Phys. Rev. A **67**, 013402 (2003).
[36]F. Buchinger, E. B. Ramsay ,E. Arnold *et al.*Phys. Rev. C **41**, 2883 (1990); **42**, 2754 (1990).
[37]B. K. Sahoo, G. Gopakumar, R. K. Chaudhuri, B. P. Das, H. Merlitz, U. Sinha Mahapatra, and D. Mukherjee, Phys. Rev. A **68**, 040501 (2003).
[38]W. Becker, W. Fisher, and H. Huhnermann, Z. Phys. A **299**, 93 (1981).
[39]B. K. Sahoo, R. K. Chaudhuri, B. P. Das, H. Merlitz, and D. Mukherjee (to be submitted).
[40]A. Roth and G. Werth, J. Phys. D **9**, 265 (1988).
[41]M. Gaillard, H. J. Plöhn, H. J. Andra, D. Kaiser, and H. H. Schluz, in *Beam-Foil Spectroscopy*, edited by I. A. Sellin and D. J. Pegg (Plenum, New York, 1976), Vol. 2, p. 853.
[42]H. J. Andra, in *Beam-Foil Spectroscopy*, edited by I. A. Sellin and D. J. Pegg (Plenum, New York, 1976), Vol. 2, p. 835.
[43]K. T. Cheng and W. J. Child, Phys. Rev. A **31**, 2775 (1995).
[44]I. Lindgren and A. Rosen, Case Stud. At. Phys. **4**, 197 (1974).
[45]L. I. Sobelman, *Introduction to the Theory of Atomic Spectra* (Pergamon, Oxford, 1972).